Journal of Engineering Mathematics **26**: 539–555, 1992.

A composite cavity model for axisymmetric high Reynolds number separated flow I: modelling and analysis

P. WILMOTT[1] and A.D. FITT[2]

[1]*Mathematical Institute, 24–29 St. Giles, Oxford OX1 3LB, UK*
[2]*Faculty of Mathematical Studies, University of Southampton SO9 5NH, UK*

Received 25 September 1991; accepted in revised form 15 May 1992

Abstract. A model is proposed for the separated high Reynolds number flow past a three-dimensional slender axisymmetric body. The current 'composite' model assumes that the separated region consists of both a region of constant pressure and a Prandtl–Batchelor region. Matched asymptotic expansions are employed to recover a nonlinear integro-differential equation for the shape of the separated region. Asymptotic solutions of this equation are obtained, and predictions for the pressure profile behind the body are given.

1. Introduction

Classical models for separated high Reynolds number flows in two dimensions come in at least two forms. First, the constant pressure Helmholtz–Kirchhoff model and second, the constant vorticity Prandtl–Batchelor model. These models are both very simple and elegant but have the important drawback that they show poor agreement with experiment. Recently O'Malley et al. (1991) proposed a physically more realistic composite model which combines the two classical ideas whilst retaining their simplicity and elegance. This model was shown to give good agreement with experiment. This is the motivation for the present study where the work is extended to the axisymmetric case.

In the two-dimensional model mentioned above, the separated region was assumed to consist of a region of constant pressure immediately behind the obstacle, and, further downstream, a Prandtl–Batchelor region, where the vorticity was constant. In the axisymmetric case we propose a similar structure for the separated region behind a blunt-based slender body, (see Fig. 1). Use must be made of the classical result, which indicates that, for an axisymmetric flow, the correct interpretation of a Prandtl–Batchelor region (a region in the flow bounded by closed streamlines) is that the vorticity is proportional to the radial distance r rather than constant. An example of such a flow in an $O(1)$ geometry is the Hill's spherical vortex (Hill (1894)).

The two-dimensional model of O'Malley et al. was justified by an appeal to experimental results. These experiments (e.g. Narayanan et al. (1974)), for high Reynolds number flow down a backward-facing step, clearly show a region of constant pressure immediately downstream of the step. The width of the region was the same order as the height of the step but the length was typically longer than the step height by a factor of ten. Hence a thin body approximation was proposed. For axisymmetric flows the experimental work is dominated by $O(1)$ Mach number compressible flows or $O(1)$ geometries. The former has obvious military applications, whilst the latter is at least in part due to experimental difficulties with the process of setting up slender axisymmetric flows and measuring their downstream pressure

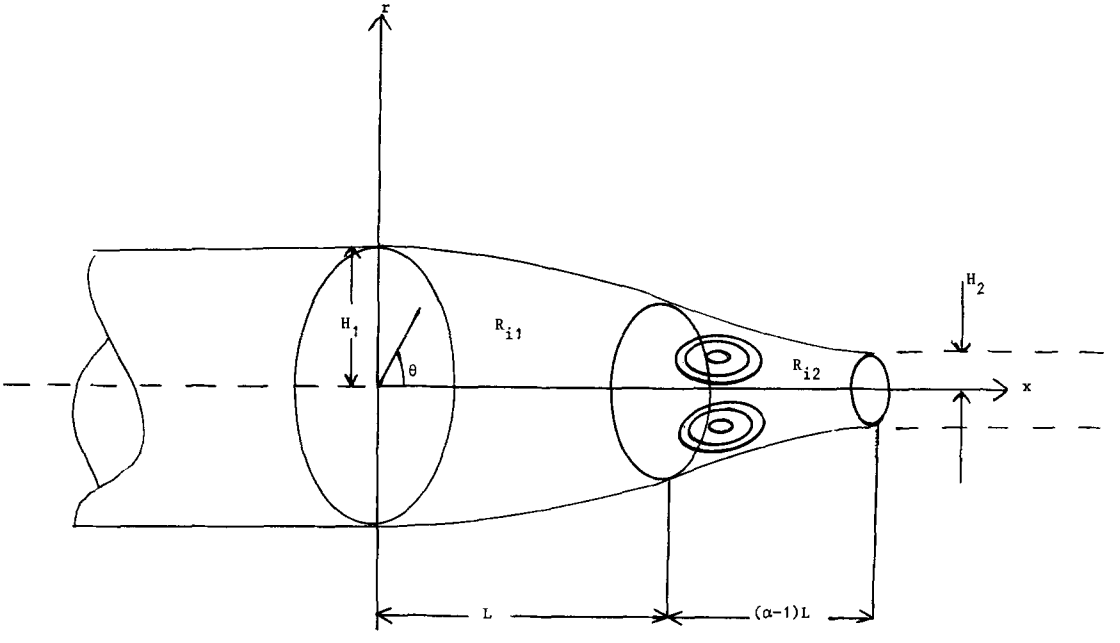

Fig. 1. Definition sketch showing the separating stream surface, stagnant zone R_{i1}, Prandtl–Batchelor region R_{i2} and equivalent afterbody.

distributions. However, we can gain some insight from this work concerning the possible flow behaviour for an axisymmetric, slender, high Reynolds number, incompressible flow.

The first point to note concerning the model presented below is the constant pressure, stagnant zone immediately downstream of the base of the slender obstacle. Such constant pressure cavities (Helmholtz–Kirchhoff models) are a common modelling assumption for separated flows (see, for example Levinson (1946) for the asymptotic behaviour of an infinite cavity far downstream) and are often observed in experimental results for two-dimensional flow down a step. For axisymmetric flows the reader is referred to Calvert (1967) and Presz & Pitkin (1974) for experimental pressure profiles. Although these experiments were conducted at $O(1)$ subsonic Mach numbers or using $O(1)$ geometries, the downstream pressure distribution shows qualitative agreement with incompressible two-dimensional flows. In Fig. 2 we have superimposed the axial pressure profile for flow past an inclined disc, taken from Calvert and the wall pressure profile for flow down a step, taken from O'Malley et al. The two profiles are not directly comparable, but the essential similarities may be easily observed. Of particular interest is the experimental work of Atli (1989) that considers axisymmetric, high Reynolds number flow at low Mach number. Although the cavity in these experiments is not slender, many of the features of the current model are present, including the recirculating region.

The second point to note is the rotational region of flow behind the obstacle. Again, this is difficult to measure experimentally and our justification this time comes from the numerical work of Fornberg (1988). Here it is found that for large Reynolds numbers the wake behind a sphere approaches the limit of a Hill's spherical vortex. We conjecture therefore that for a flow past a *slender* axisymmetric body the equivalent limit would be a Prandtl–Batchelor region with large aspect ratio.

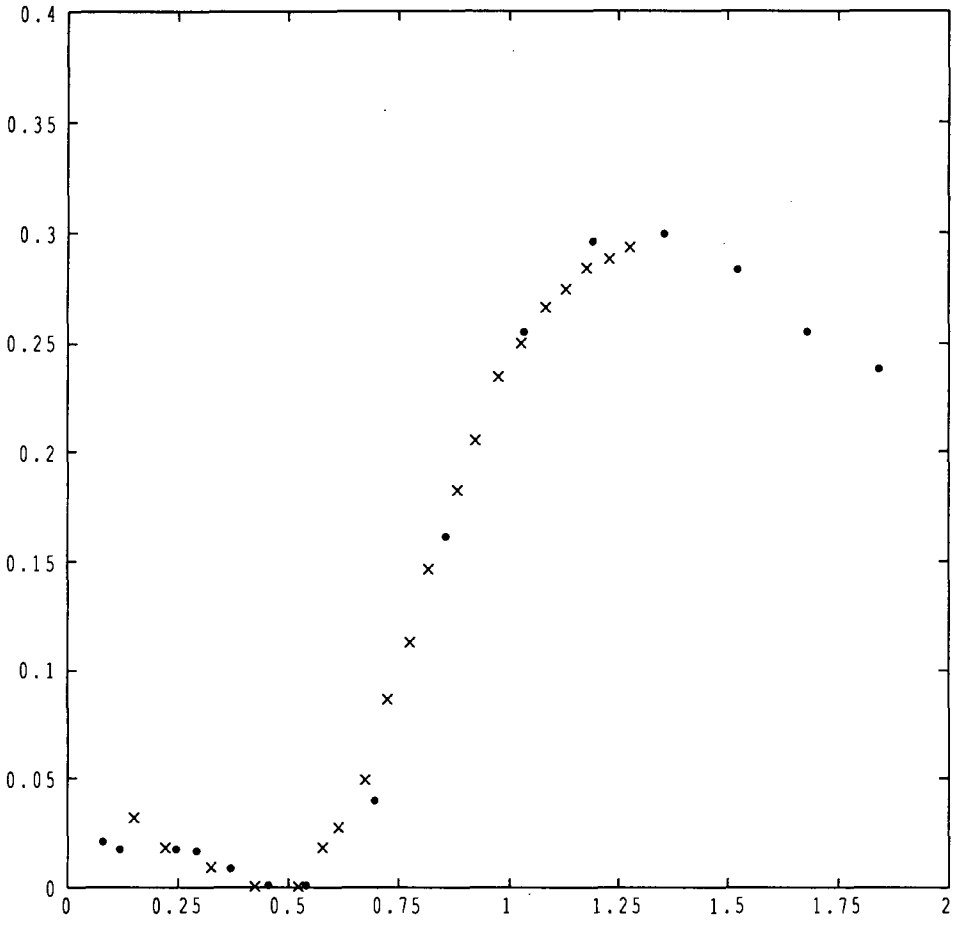

Fig. 2. Axial pressure profile for flow past an inclined disk (Calvert (1967) ×) and wall pressure profile for flow down a step (O'Malley et al. (1991) ●). (Arbitrary Units.)

Finally, we refer to work by Cumberbatch & Wu (1961), Sadovskii (1971) and Bliss (1982), all of which have some of the characteristics of our proposed model.

Cumberbatch & Wu consider the separated flow past a slender, triangular plate hydrofoil. Within the separated region the flow is stagnant and the pressure is uniform. The hydrofoil is at a small angle of attack and separation occurs at its leading edge. The flow is not axisymmetric and they close the cavity above by adopting a Riabouchinsky model. Downstream of the hydrofoil the cavity is assumed to have only a small effect on the flow near the hydrofoil. This allows them to calculate the lift and drag on the plate. Our approach extends their work in two ways. First, we have a physically more realistic model for the cavity and, second, we allow the cavity to play the major role in determining the flow and hence the pressure on the body.

Sadovskii considers an isolated rotational flow in two dimensions, symmetric about an axis. In this model there is a separating streamline within which the vorticity is constant and outside of which the vorticity is zero. A family of solutions is found depending upon the jump in Bernoulli constant across the separating streamline. When this constant is non-zero, the region of constant vorticity has a cusped closure. Although this work has not been

extended to the axisymmetric case (the existence of axisymmetric closed Prandtl–Batchelor regions is still an important open question) we conjecture that similar rotational flows are possible. When there is no jump in the Bernoulli constant the flow would correspond to that of a Hill's spherical vortex. However, with a jump we expect a cusped closure, so that the pressure along the separating streamline remains continuous.

Bliss considers the flow through a single slot of finite length in a wall separating a uniform free stream and a quiescent fluid at a different static pressure, his study being motivated by the need to understand the aerodynamic behaviour of slots which are used in the walls of transonic wind tunnels. Slender body theory and matched asymptotic expansions are used to produce an integro-differential equation for the unknown position of the free surface. When the displacement of the free surface is small compared to the slot width, a linear integro-differential equation describes the free surface shape and may be solved analytically for certain slot planforms. This model differs from ours in that the free surface is never required to reattach and the pressure in the slot is uniform – there is no recirculating zone.

In section 2 we present our model and derive a nonlinear integro-differential equation for the cavity cross-sectional area using asymptotic analysis based upon the slenderness parameter. In section 3 a comparison is made with the properties of the two-dimensional equation. This is followed by the derivation of some consistency conditions for the equation and some discussion concerning the closure of the cavity. In section 4 we consider a further asymptotic limit for which some analytic solutions are possible. Conclusions are drawn in section 5 and scope for further work is discussed. The numerical solution and further analysis is contained in a companion paper (Fitt & Wilmott (1992)).

2. The axisymmetric cavity

We consider steady, laminar, inviscid, incompressible flow past an axisymmetric cavity with axes r, θ and x as shown in Fig. 1. We denote unit vectors in the x, r and θ directions by $\mathbf{e}_x$, $\mathbf{e}_r$ and $\mathbf{e}_\theta$ respectively. Far away from the cavity the undisturbed flow is assumed to have constant speed U_∞ in the positive x-direction, the cavity has length αL (where α is an order (1) constant to be determined; the reason for this definition of the length will become apparent later) and typical width H_1. We assume that the cavity has been produced by an obstruction in the flow which may be a finite axisymmetric solid body or may also be thought of as being a semi-infinite obstruction (for example a cylinder) which stretches along the negative x-axis from $x = 0$ to $x = -\infty$.

The flow outside the cavity 'sees' two types of boundary, that is, the fixed boundary of the obstacle, and the free boundary of the cavity, whose position is not known. Here, we consider the simplest case where point of separation from the obstacle is known *a priori*; namely a semi-infinite cylinder of radius H_1 whose axis is aligned with the flow, so that separation is from the rear of the cylinder.

We shall permit the cavity to join onto a cylindrical Riabouchinsky type of afterbody (see Fig. 1). There are two reasons for this. First, it will be necessary to reattach to a solid body to ensure cusped closure of the cavity and hence continuity of pressure. Second, it was found that such an imaginary afterbody produced better agreement with experiment in the case of two-dimensional flow down a step. In this case the afterbody was interpreted as a model for the growing shear layer downstream of the cavity. Such a wake region is expected to exist in

an axisymmetric flow also; following O'Malley et al. we shall call this the equivalent afterbody. These two points will be discussed more fully in section 3.

Assuming that outside the cavity the flow is irrotational with velocity $\mathbf{q} = u\mathbf{e}_x + v\mathbf{e}_r$ and velocity potential Φ, the axisymmetry allows us to assume that Φ is a function of x and r alone. Denoting the boundary of the cavity by $r = R(x)$, and assuming that $R(0) = H_1$, $R(\alpha L) = H_2$, the radius of the afterbody, the full (dimensional) problem for the flow outside the obstruction/cavity combination is

$$\begin{cases} \Delta\Phi = 0 & \\ \Phi \sim U_\infty x & \text{as } |\mathbf{x}| \to \infty \\ (\mathbf{q}\cdot\nabla)[r - R(x)] = 0 & \text{on } r = R(x) \\ \frac{1}{2}|\nabla\Phi|^2 = \frac{1}{2}U_\infty^2 + (p_\infty - p_{\text{cav}})/\rho & \text{on } r = R(x)\,. \end{cases}$$

Here p_∞ and ρ denote the pressure in the undisturbed free stream and the density of the fluid respectively, and p_{cav} is the pressure on the boundary $r = R(x)$ which in general will be a function of x. The boundary conditions are of a standard type for elliptic operators; the presence of both a kinematic and a dynamic condition on $r = R(x)$ reflects the fact that the position of the boundary is unknown and must be determined as part of the solution. (Of course for $x < 0$ and $x > \alpha L$ we regard the shape of the body as known.)

2.1. *The slender cavity*

Having formulated the problem for an arbitrary cavity behind a cylinder, we now focus attention on the case where the cavity is slender so that $H_1/L \ll 1$.

Outside the cavity we first subtract off the free stream flow and non-dimensionalize by setting

$$x = L\hat{x}\,, \quad r = L\hat{r} \quad \text{and} \quad \Phi = U_\infty x + \varepsilon^2 L U_\infty \hat{\phi}\,.$$

Here the hats denote non-dimensional variables outside the cavity and the quantity $\varepsilon \ll 1$ is a small parameter of algebraic order H_1/L. (The reason for not immediately defining ε to be *equal* to H_1/L will become apparent later.) It is also worth mentioning at this point that although the disturbance potential has been assumed to be of $O(\varepsilon^2)$, the formulation of the problem within the cavity will inevitably lead to the appearance of terms involving $\log(\varepsilon)$, so all the unknown quantities will implicitly be assumed to be functions of $\hat{x}$, $\hat{r}$ and $\log(\varepsilon)$.

We shall employ the technique of matched asymptotic expansions to examine the flow, and so we define an outer region which is composed of points at an $O(1)$ distance away from the cavity and an inner region where distances from the cavity are of the order of its typical radius.

The outer solution

The velocity potential in the outer region is most easily represented by a distribution of sources along the axis of the cavity so that (dropping the hats) we have

$$\phi = \int_0^\alpha \frac{C(\xi)\,\mathrm{d}\xi}{\sqrt{(x-\xi)^2 + r^2}}\,, \tag{1}$$

where the function C is to be determined. If the obstacle had a cross-section of varying area

then we could also introduce a distribution of sources along the negative x-axis. We do not consider this case here, however.

The inner solution

In the inner region we rescale the radial coordinate by writing $r = \varepsilon r^*$. Now the inner velocity potential, ϕ^* say, must satisfy the radial Laplacian

$$\phi^*_{r^*r^*} + \frac{1}{r^*}\,\phi^*_{r^*} = 0$$

to leading order together with the leading term in the Bernoulli pressure condition

$$\phi^*_{x^*} + \frac{1}{2}\,\phi^{*2}_{r^*} = \frac{p_\infty - p_{\text{cav}}}{\rho\varepsilon^2 U_\infty^2} \quad \text{on } r^* = R^*\,,$$

where $R = \varepsilon L R^*$ and the kinematic condition $\phi^*_{r^*} = R^{*\prime}$ where $' = \mathrm{d}/\mathrm{d}x^*$. Clearly the solution for ϕ^* is

$$\phi^* = A(x)\log r^* + B(x)\,,$$

so that A and B must satisfy

$$A = R^* R^{*\prime}$$

and

$$A' \log R^* + B' + \frac{1}{2}\,\frac{A^2}{R^{*2}} = \frac{p_\infty - p_{\text{cav}}}{\rho\varepsilon^2 U_\infty^2}\,. \tag{2}$$

The matching condition

Writing (1) in inner variables ($r = \varepsilon r^*$) and expanding for small ε, we find that

$$\phi = -2C\log r^* + C\log\left(\frac{4x(\alpha - x)}{\varepsilon^2}\right) + \int_0^\alpha \frac{C(\xi) - C(x)\,\mathrm{d}\xi}{|x - \xi|}\,.$$

Therefore

$$C = -2A\,,$$

(to balance the $\log r^*$ terms) and

$$B = C\log\left(\frac{4x(\alpha - x)}{\varepsilon^2}\right) + \int_0^\alpha \frac{C(\xi) - C(x)\,\mathrm{d}\xi}{|x - \xi|}\,.$$

Note that the source strength C is proportional to the rate of change of the cross-sectional area of the cavity.

The model is now fully posed as an integro-differential equation for the cavity profile, provided that we can model the pressure within the cavity, p_{cav}.

The interior problem

We must now examine the flow inside the cavity. In the introduction we have discussed the experimental evidence concerning the flow behaviour in the wake of a slender obstacle. This evidence is strengthened by experimental work on equivalent two-dimensional separated flows and we thus present here an axisymmetric model analogous to that of O'Malley et al. The model is inviscid, with the effects of viscosity assumed to be confined to narrow shear layers (for example, emanating from the rim of the base of the obstacle). It is possible that the flow contains many eddies, perhaps of ever decreasing size and alternating direction as the base of the obstacle is approached and/or further downstream. Our present model may thus be thought of as the simplest possible and, since it cannot be expected to capture the full structure of the real flow, we may interpret our vorticity as a spatial and temporal average of the actual vorticity.

The flow within the cavity ($r^* < R^*$) is modelled as follows. In region R_{i1} (see figure 1), which is that part of the cavity immediately downstream of the base of the obstacle, we assume that the flow is stagnant. This is the classical Helmholtz–Kirchhoff model having $p_{\text{cav}} = p_c = \text{constant}$. For this model it is found to be impossible to enforce cusped closure (for a finite cavity) at reattachment, and the pressure is therefore discontinuous. The Helmholtz–Kirchhoff cavity is thus often taken to be infinite in length (with p_c representing the pressure at infinity in the free stream) or to reattach to an image body at a finite distance downstream (the Riabouchinsky model). Here we shall adopt an alternative approach. We restrict the stagnant region to the interval $0 \leqslant x \leqslant 1$ and, for $1 \leqslant x \leqslant \alpha$ we assume that the remainder of the cavity is a Prandtl–Batchelor region of rotational flow. In this region (labelled R_{i2} in Fig. 1), the vorticity is essentially known (but see below for a discussion of axisymmetric flows bounded by closed streamlines). We have seen in the introduction how this model is suggested by the numerical work of Fornberg. Note that in the current model the cavity aspect ratio is $1/\varepsilon$ and the cavity is thus slender. For this reason the details of how the regions R_{i1} and R_{i2} are joined at their interface need not concern us, since we expect this to occur over a distance of $O(\varepsilon)$ which is small compared to the length of the cavity. We shall be content to insist upon the continuity of pressure and cavity area from $x = 1-$ to $x = 1+$.

If we now define ε via

$$\varepsilon^2 = \frac{p_\infty - p_c}{\frac{1}{2}\rho U_\infty^2},$$

we find that the right hand side of (2) becomes simply 1/2. It is worth remarking that the problem could equally well have been set up by defining $\varepsilon = H_1/L$, but in an experiment the pressure coefficient inside the stagnant region immediately downstream of the beginning of the cavity would be the more natural quantity to measure, rather than L whose experimental determination would be rather hard. The quantity H_1/L is still, of course, of algebraic order ε.

Turning now to the region R_{i2}, we employ the same scalings as in R_{i1}, except for the fact that now the flow is no longer irrotational and there is no velocity potential. Accordingly we define a stream function ψ such that

$$u = \frac{1}{r^*}\,\psi_{r^*}, \qquad v = -\frac{1}{r^*}\,\psi_x$$

so that the continuity equation

$$u_x + \frac{1}{r^*}(r^* v)_{r^*} = 0$$

is identically satisfied. Having non-dimensionalized ψ by setting

$$\psi = \varepsilon^3 U_\infty L^2 \psi^* ,$$

and further scaling

$$u = \varepsilon U_\infty u^* , \qquad v = \varepsilon^2 U_\infty v^*$$

so that pressure variations of the correct order of magnitude are produced, we observe that a classical result of Batchelor (1955) concerning the distribution of vorticity in regions of flow confined by closed streamlines, relating in particular to Hill's spherical vortex, implies that the vorticity in region R_{i2} must be proportional to r^*. Accordingly we set the θ-component of vorticity equal to $-\beta r^*$ and non-dimensionalize by writing $\beta = (\varepsilon^{-1} U_\infty / L^2)\beta^*$ so that

$$\frac{\partial}{\partial r^*}\left[\frac{1}{r^*}\psi^*_{r^*}\right] = \beta^* r^*$$

to lowest order, which may easily be solved to yield

$$\psi^* = \frac{r^{*2}\beta^*}{8}[r^{*2} - R^{*2}]$$

and this solution may now be used to match across the dividing streamline and close the problem. The pressure on the boundary of R_{i2} satisfies

$$p_{i2} + \frac{1}{2}\rho \mathbf{q}_{i2}^2 + h = p_\infty + \frac{1}{2}\rho U_\infty^2 ,$$

where the constant h has been introduced to reflect the fact that owing to the presence of the infinitesimal shear layer between the free stream and the rotational region there will be a jump in the Bernoulli constant across $r^* = R^*(x)$. Using the stream function for the flow in R_{i2} we find that the non-dimensional pressure coefficient is given by

$$C_p = \frac{p_\infty - p}{\frac{1}{2}\rho U_\infty^2} = -1 + \frac{h}{\frac{1}{2}\rho U_\infty^2} + \frac{\varepsilon^2 \beta^{*2} R^{*4}}{16} .$$

Defining a non-dimensional Bernoulli jump via

$$h = \frac{\rho U_\infty^2}{2}[1 + \varepsilon^2 h^*]$$

we find that

$$C_p = \varepsilon^2 h^* + \varepsilon^2 \beta^{*2} R^{*4}/16 .$$

The matching may finally be completed by eliminating A and B and using the relevant pressure coefficients in both regions to ensure continuity of pressure across the cavity

boundary. The integral equation for $R^*(x)$ then becomes

$$\frac{\mathrm{d}}{\mathrm{d}x}\left[\frac{1}{2}R^*R^{*\prime}\log\left(\frac{\varepsilon^2}{4x(\alpha-x)}\right)-\frac{1}{2}\int_0^\alpha\frac{R^*(\xi)R^{*\prime}(\xi)-R^*(x)R^{*\prime}(x)\,\mathrm{d}\xi}{|x-\xi|}\right]$$
$$=-\frac{1}{2}R^{*\prime 2}-(R^*R^{*\prime})'\log R^*+\begin{cases}1/2 & (0\leqslant x\leqslant 1)\\ h^*+\beta^{*2}R^{*4}/16 & (1\leqslant x\leqslant\alpha)\end{cases}. \tag{3}$$

We may also take the opportunity to simplify the governing integral equation further by working in terms of the cavity area rather than the radius. Writing

$$T(x)=\pi R^{*2}(x)\,,$$

and dropping the stars for convenience, the equation becomes

$$\frac{\mathrm{d}}{\mathrm{d}x}\left[T'(x)\left(\log(\varepsilon/2)-\log\sqrt{x(\alpha-x)}\right)-\frac{1}{2}\int_0^\alpha\frac{T'(\xi)-T'(x)\,\mathrm{d}\xi}{|x-\xi|}\right]+\frac{T'^2(x)}{4T(x)}$$
$$+\frac{T''(x)}{2}\log\left(\frac{T}{\pi}\right)=\begin{cases}\pi & (0\leqslant x\leqslant 1)\\ 2\pi h+\beta^2T^2(x)/8\pi & (1\leqslant x\leqslant\alpha)\end{cases}. \tag{4}$$

We now consider boundary conditions and continuity requirements. First, an obvious requirement is that the pressure should be continuous at $x=1$. This implies that

$$h=\frac{1}{2}-\frac{\beta^2T^2(1)}{16\pi^2}\,.$$

As far as boundary conditions are concerned, we have

$$T(0)=\frac{\pi H_1^2}{\varepsilon^2L^2}\,,\qquad T(\alpha)=\frac{\pi H_2^2}{\varepsilon^2L^2}\,,$$

whilst for smooth separation and reattachment we also require

$$T'(0)=T'(\alpha)=0\,.$$

3. Some comments on the integro-differential equation

Before dealing with some of the properties of (4), it is worth noting that there are a number of different ways of writing the equation using various conditions at the boundaries. Firstly, if the integral is split into two portions, then integrated by parts and differentiated, we find that the equation may be written

$$-\frac{1}{2}\int_0^\alpha\frac{T''(\xi)-T''(x)\,\mathrm{d}\xi}{|\xi-x|}+\frac{T''(x)}{2}\log\left[\frac{\varepsilon^2T(x)}{4\pi x(\alpha-x)}\right]$$
$$+\frac{T'^2(x)}{4T(x)}=\begin{cases}\pi & (0\leqslant x\leqslant 1)\\ \pi-\frac{\beta^2}{8\pi}\left[T^2(1)-T^2(x)\right] & (1\leqslant x\leqslant\alpha)\end{cases} \tag{5}$$

with

$$T(0) = \frac{\pi H_1^2}{\varepsilon^2 L^2}, \qquad T(\alpha) = \frac{\pi H_2^2}{\varepsilon^2 L^2}, \qquad T'(0) = T'(\alpha) = 0.$$

We shall show shortly that if $T(\alpha) \neq 0$ then $T''(0) = T''(\alpha) = 0$, in which case another integration by parts may then be performed to allow the equation to be rewritten as

$$\frac{1}{2}\int_0^\alpha T'''(\xi)\,\mathrm{sgn}(\xi - x)\log|\xi - x|\,\mathrm{d}\xi + \frac{T''(x)}{2}\log\left[\frac{\varepsilon^2 T(x)}{4\pi}\right] + \frac{T'^2(x)}{4T(x)} = \begin{cases} \pi & (0 \leq x \leq 1) \\ \pi - \frac{\beta^2}{8\pi}[T^2(1) - T^2(x)] & (1 \leq x \leq \alpha) \end{cases} \tag{6}$$

with

$$T(0) = \frac{\pi H_1^2}{\varepsilon^2 L^2}, \qquad T(\alpha) = \frac{\pi H_2^2}{\varepsilon^2 L^2}, \qquad T'(0) = T'(\alpha) = 0.$$

Each of these forms of the equation has its advantages, but (5) is probably the easiest to manipulate.

3.1. Comparison with the model of O'Malley et al.

We recall that the analogous equation for the free boundary in the two-dimensional problem (see O'Malley et al. (1991)) is

$$\frac{1}{\pi}\int_0^\alpha \frac{S'(\xi)}{x - \xi}\,\mathrm{d}\xi = \begin{cases} \frac{1}{2} & (0 \leq x \leq 1) \\ \frac{1}{2} - \frac{\omega^2}{8}(S^2(1) - S^2(x)) & (1 \leq x \leq \alpha) \end{cases}, \tag{7}$$

where $S(x)$ represents the height of the separating streamline. (This may be thought of as an extension of the model of Childress (1966) who assumed the cavity to be composed of a single region in which the vorticity was constant.) The structure of (5) and (7) are very similar, but differ in two main respects; first, the nonlinear term in Bernoulli's equation only makes an appearance in the three-dimensional model (giving rise to the term $T'^2/4T$) and, second, the slenderness parameter ε appears explicitly in the $\log \varepsilon$ term. The latter is very common in integral equations from Laplace's equation in an axisymmetric geometry. At first glance it might appear that the integral equation (5) possesses one more derivative than (7). That this is not actually the case may be seen by integrating (7) by parts. Now (7) takes the form

$$\frac{1}{\pi}\int_0^\alpha S''(\xi)\log|x - \xi|\,\mathrm{d}\xi = \begin{cases} \frac{1}{2} & (0 \leq x \leq 1) \\ \frac{1}{2} - \frac{\omega^2}{8}(S^2(1) - S^2(x)) & (1 \leq x \leq \alpha) \end{cases}. \tag{8}$$

The two forms (5) and (8) are only now directly comparable since the two kernels each correspond to the potential for a source evaluated on the x-axis.

3.2. Consistency conditions for the equation

It was found by Childress using a force balance argument for the two-dimensional problem that the parameters in (7) are not all independent. This was also shown by O'Malley et al.

using a simpler argument. A similar analysis is applicable in the present case. A succinct result may be derived by multiplying the equation (5) through by $T'(x)$ and integrating from 0 to α with respect to x. This allows the whole of the right hand side and much of the left hand side of the equation to be integrated immediately, leaving

$$\frac{1}{2}\int_0^\alpha \left[T''(x)T'(x)\log(x(\alpha-x)) + T'(x)\left(\int_0^\alpha \frac{T''(\xi)-T''(x)}{|\xi-x|}\,\mathrm{d}\xi\right)\right]\mathrm{d}x$$

$$= \pi(T(\alpha)-T(0)) - \frac{\beta^2}{8\pi}\left(T^2(1)T(\alpha) - \frac{T^3(\alpha)}{3} - \frac{2T^2(1)}{3}\right).$$

An integration by parts shows that the left hand side is identically zero, so that

$$\beta^2 = \frac{8\pi^2(T(\alpha)-T(0))}{T^2(1)T(\alpha) - \frac{1}{3}T^3(\alpha) - \frac{2}{3}T^3(1)}\,. \tag{9}$$

This result effectively relates the vortex strength to the height of the obstacle and the length of the constant pressure region. Similar relationships between parameters can be found in many integral equations of the above form (or its two-dimensional analogue); see, for example O'Malley et al.

As in the two-dimensional case, it is also possible to derive a second consistency condition. First, we note that the integral term in the equation (5) vanishes identically when integrated with respect to x from 0 to α. This gives

$$\int_0^\alpha \frac{T''(x)}{2}\left[\frac{1}{2}\log T(x) + \log\left(\frac{\varepsilon^2}{4\pi x(\alpha-x)}\right)\mathrm{d}x\right] = \pi\alpha - \int_1^\alpha \frac{\beta^2}{8\pi}\left[T^2(1)-T^2(x)\right]\mathrm{d}x\,. \tag{10}$$

The equivalent result in the two-dimensional case (O'Malley et al.) was found to be useful in the numerical solution of the corresponding integral equation. Of course, any number of consistency conditions may be found by multiplying the equation by suitable functions and integrating. Equation (9) is particularly useful since it effectively eliminates a parameter ($T(1)$ or β, say). (In practice, $T'(0)=0$ together with (9) ensure that $T'(\alpha)=0$.)

3.3. *Cavity closure*

We shall now briefly examine the behaviour of the separating streamline in the neighbourhood of $x=0$ and $x=\alpha$ and then discuss the consequences.

In order to examine this local behaviour we need to determine which of the terms in (4) play an important role near singularities. Consider the neighbourhood of $x=0$. Clearly the terms $\frac{\mathrm{d}}{\mathrm{d}x}(T'\log(\varepsilon/2))$ and $T''\log(T/\pi)$ are always small compared to $\frac{\mathrm{d}}{\mathrm{d}x}(-T'\log x)$. We may also neglect the term $T'^2/4T$ since $T(0)$ is finite and $T'(0)=0$. We may explicitly perform the differentiation in (4) with respect to x (taking care with the differentiation of the integral term). Then, after writing $T'(0)=0$ and $T'(\alpha)=0$ we find that we must balance, near $x=0$, two out of the three terms in

$$\int_0^\alpha \frac{f(\xi)-f(x)\,\mathrm{d}\xi}{|\xi-x|} + f(x)\log x = -2\pi\,, \tag{11}$$

where $f(x)=T''(x)$.

We can eliminate only the balance between the last two terms. For suppose that locally $f(x) \sim -2\pi/\log(x)$, then substitution of such a local behaviour into the integral, terms in (11) gives a function with local behaviour $\log(-\log x)$, which is singular at $x = 0$. Both the other two combinations of two out of the three terms are permitted. First, a balance between the first and last terms will be possible provided $f(x)\log(x) \to 0$ as $x \to 0$, allowing for example $f(x) \sim ax^{\mu}$, $\mu > 0$. Unfortunately, neither a nor μ may be determined explicitly since the balance of terms is global rather than local. The second possibility is a balance between the integral term and the log term in (11) in such a way that both are individually infinite at $x = 0$ but cancel each other out. In this case we find that

$$f(x) \sim a(-\log x)^{-1/2}$$

where again a is determined via a global problem. Thus we conclude that in either case $T''(0) = 0$. The argument carries over directly to the neighbourhood of $x = \alpha$ provided that $T(\alpha) \neq 0$ and again we find that $T''(\alpha) = 0$. In the special case $T(\alpha) = 0$, the term $T''(x)\log T$ in (4) becomes important and we cannot rule out the possibility that $T''(\alpha)$ is infinite.

The importance of the second derivative of $T(x)$ may be appreciated by considering the pressure distribution. For $x < 0$ and $x > \alpha$ the pressure acting on the obstacle or afterbody is given by

$$p = -\frac{1}{2}\frac{\mathrm{d}}{\mathrm{d}x}\int_0^{\alpha} \frac{T'(\xi)\,\mathrm{d}\xi}{|x-\xi|}\,.$$

The pressure will thus be infinite at an end of the cavity where $T''(x) \neq 0$. Furthermore, since the cavity radius is $\sqrt{T(x)}$, a cavity having $T(\alpha) = 0$ will only be cusped if $T''(\alpha) = 0$.

Clearly, we know that the pressure will remain finite if we insist on an afterbody so that $T(\alpha) \neq 0$. However, this is somewhat unsatisfactory since we would like the freedom to ignore the afterbody. We shall argue that the infinite pressure for $T(\alpha) = 0$ is an artefact of our model which can be eliminated by a better local analysis.

First, observe that it appears that slender body theory requires continuity of $T''(x)$ for finite pressure whereas thin aerofoil theory only requires the continuity of $S'(x)$. The latter is not unreasonable since a discontinuity in slope leads to a stagnation point or a point of infinite velocity and hence pressures which are not close to the pressure at infinity. This manifests itself in thin aerofoil theory as an infinite pressure at points of discontinuous gradient. This would also be expected to be true for a slender body – discontinuous area gradient should also lead to infinite pressure locally. However, for an axisymmetric body with continuous area gradient the flow is evidently locally two-dimensional (on a scale small compared with the radius of the body) and should therefore have finite pressure. Our first conclusion is thus that the simple slender body theory used here breaks down near discontinuities of $T''(x)$. However, if $T(\alpha) = 0$ we must still have $T''(\alpha) = 0$ otherwise the closure will be at best conical, and the pressure locally infinite.

Recall the analogous situation for a two-dimensional Helmholtz–Kirchhoff flow. A thin aerofoil type of approximation for such a model cannot guarantee cusped closure – in fact the separating streamline generally reattaches normally. However this does not discredit the constant pressure model since it is well known that there are $O(1)$ geometries which do permit cusped closure (e.g. the well known Lighthill cavity (Lighthill (1945)). The real reason that constant pressure models are inadequate (apart from giving poor agreement with

experiment) is that they cannot be both cusped and convex – the latter being a requirement that the pressure must be increasing away from the cavity. Fortunately, for our problem, we know that there exist two-dimensional $O(1)$ geometry Sadovskii vortices which have all the local and global properties we require and, as mentioned in the introduction, we expect similar confined vorticity flows to exist in three dimensions. Such a vortex would then be the local behaviour for our cavity near $x = \alpha$ in the case $T(\alpha) = 0$. Thus if we were to choose $T(\alpha) = 0$ then we could improve our model by a more careful local analysis near $x = \alpha$ and by employing a more sophisticated slender body theory (see Handelsman & Keller (1967)). We shall not pursue this point further here.

4. The limit $\log \varepsilon \to -\infty$

It is of interest to examine the solution to the governing equations in the case $\log \varepsilon \to -\infty$ since further analysis is then possible. Otherwise the solution of (5) may only be obtained by numerical means. (See Fitt & Wilmott (1992).) Note that we expect qualitatively similar results for the two cases where $\log \varepsilon$ is finite and where $\log \varepsilon \to -\infty$. We also find that qualitative comparison is possible between the $\log \varepsilon \to -\infty$ limit and the two dimensional solution.

Making the obvious scalings

$$T(x) = \frac{U(x)}{-\log \varepsilon}, \qquad \beta = -\gamma \log \varepsilon,$$

the leading order problem becomes

$$-U''(x) = \begin{cases} \pi & (0 \leqslant x \leqslant 1) \\ \pi - \frac{\gamma^2}{8\pi}[U^2(1) - U^2(x)] & (1 \leqslant x \leqslant \alpha) \end{cases}.$$

At $x = 0$ we have

$$T(0) = \frac{\pi H_1^2}{\varepsilon^2 L^2}$$

and so

$$U(0) = -(\log \varepsilon)\frac{\pi H_1^2}{\varepsilon^2 L^2} = D_1,$$

which we assume to be $O(1)$. (Hence our insistence that H_1/L is of *algebraic* order ε; it must actually be $O(\varepsilon/(-\log \varepsilon)^{1/2})$.) We shall also insist that $U'(0) = U'(\alpha) = 0$ and $U(\alpha) = D_2$. Thus

$$U(x) = D_1 - \frac{\pi x^2}{2} \quad (0 \leqslant x \leqslant 1),$$

and for $1 \leqslant x \leqslant \alpha$

$$\alpha - x = \int_{D_2}^{U(x)} \frac{\mathrm{d}\xi}{\sqrt{-P\xi^3 + Q\xi + R}}$$

where

$$P = \frac{\gamma^2}{12\pi}, \qquad Q = -2\pi + \frac{\gamma^2 U(1)^2}{4\pi}, \qquad R = 2\pi U(\alpha) - \frac{\gamma^2}{4\pi}\left(U(1)^2 U(\alpha) - \frac{U(\alpha)^3}{3}\right).$$

Continuity of $U(x)$ at $x = 1$ then gives us the following relationship between α, γ, D_1 and D_2

$$\alpha - 1 = \int_{D_2}^{D_1 - \pi/2} \frac{d\xi}{\sqrt{-P\xi^3 + Q\xi + R}}.$$

Continuity of $U'(x)$ at $x = 1$ then leads to

$$D_2 - D_1 = \frac{\gamma^2}{8\pi^2}\left(D_2(D_1 - \pi/2)^2 - \tfrac{1}{3}D_2^3 - \frac{2}{3}(D_1 - \pi/2)^3\right).$$

This latter equation is identical to that given by the first consistency condition (9). The important points to note about the $\log \varepsilon \to -\infty$ limit concern the role of the integral in (5) and the behaviour near the end points of the cavity, and the dimensionality.

First, we saw in section 3.3 how the solution to the full integral equation (5) has $T''(0) = T''(\alpha) = 0$. We identified the decay of $T''(x)$ at the two ends to be either x^μ for some $\mu > 0$ or $(-\log x)^{-1/2}$. In the former case the balance of terms was between the integral and constant terms, in the latter there was a balance between the integral and $T'' \log x$. This subtle behaviour has been lost in the $\log \varepsilon \to -\infty$ limit since both the integral and the $T'' \log x$ term have been discarded by dint of being small compared with the $T'' \log \varepsilon$ term.

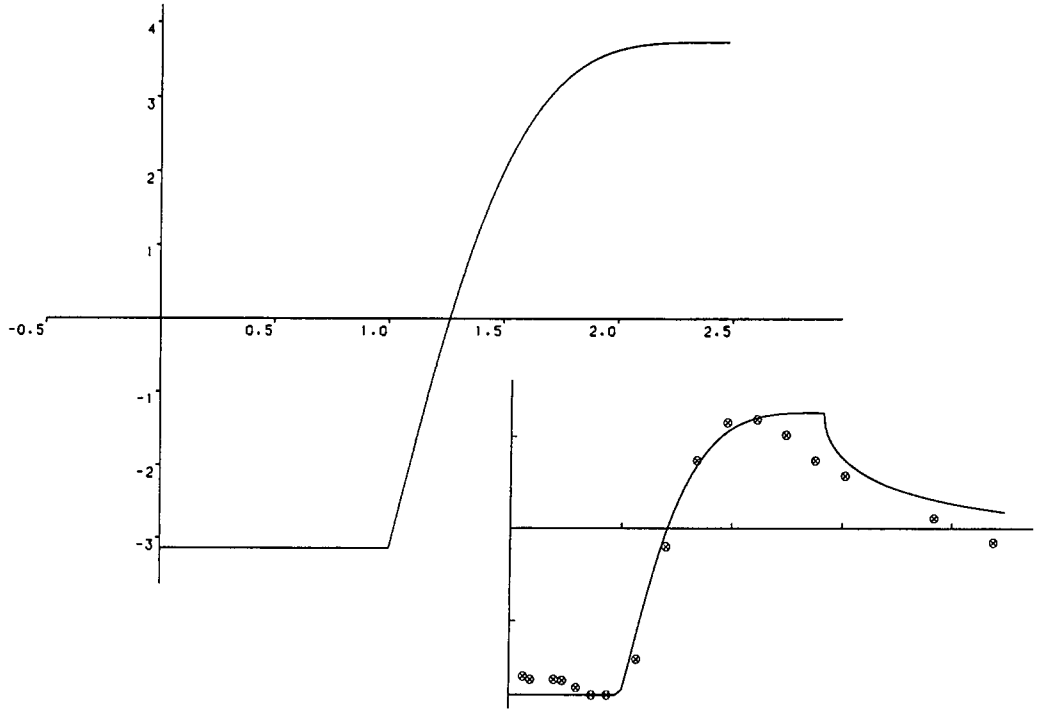

Fig. 3a. The pressure profile in the case $\log \varepsilon \to -\infty$ with $D_1 = 5$ and $D_2 = 0$. ($\alpha = 2.4741$.) (Inset: A typical pressure profile for flow down a step, experimental and theoretical (O'Malley et al. 1991).)

As a consequence we see that our solution for $U(x)$ does not have $U''(x) = 0$ at the ends of the cavity. Hence the pressure outside the cavity, along the x-axis, becomes infinite at $x = 0, \alpha$. However, this is only infinite as far as the pressure away from the two ends is concerned; a local analysis would show that the $O(-1/\log \varepsilon)$ outer pressure matches with an $O(1)$ interior pressure.

Secondly, our example illustrates the dimensionality of the full problem since there are four physical parameters α, D_1, γ and D_2 (which can be identified as cavity length, width, vorticity and afterbody height) with two relationships between them. This suggests the dimensionality of the equation (5) together with its boundary conditions is three since $\log \varepsilon$ does not scale out of (5).

Since we cannot have $U''(\alpha) = 0$ with the $\log \varepsilon \to -\infty$ limit we may as well consider as an example the simplest case $D_2 = 0$, that is, there is no afterbody.

In Figs 3(a), (b) and (c) we plot the pressure, the scaled cross-sectional area $U(x)^{1/2}$ and the cavity width $U(x)$ for $D_1 = 5$ and $D_2 = 0$. In this case we find that $\alpha = 2.4741$. In Fig. 3a the pressure is shown as zero for x outside $[0, \alpha]$, of course, the above analysis shows it to be

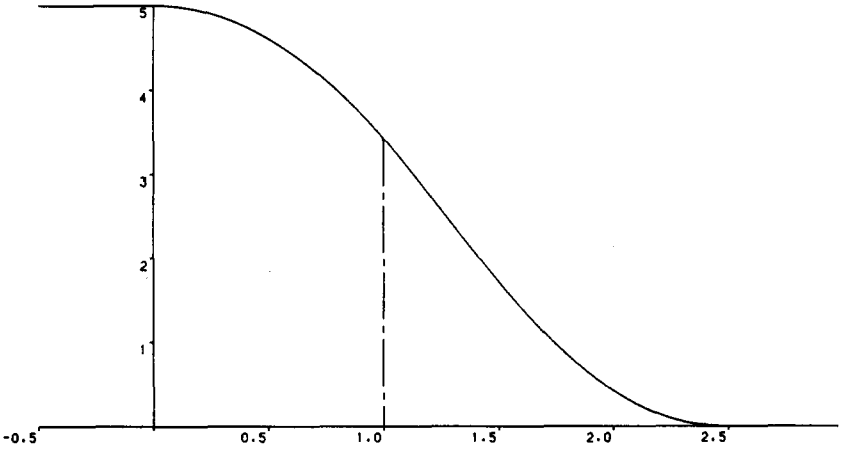

Fig. 3b. Cavity cross-sectional area for the limit $\log \varepsilon \to -\infty$ with $D_1 = 5$ and $D_2 = 0$.

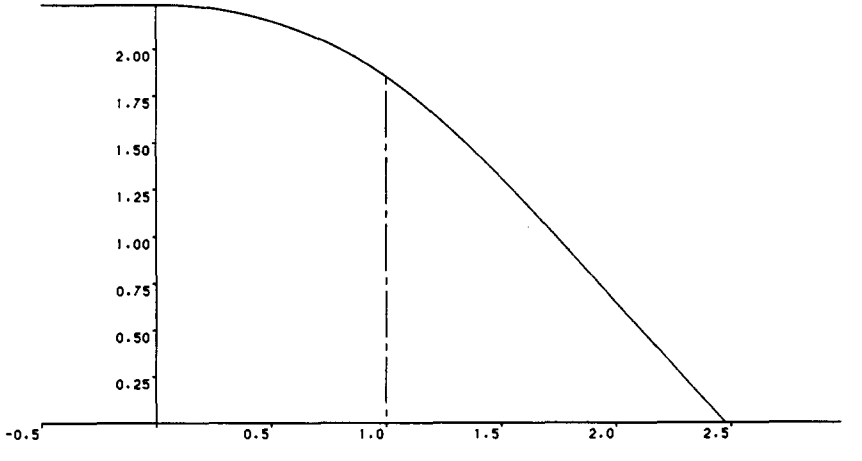

Fig. 3c. Cavity width for the limit $\log \varepsilon \to -\infty$ with $D_1 = 5$ and $D_2 = 0$.

$O(-1/\log \varepsilon)$. Inset in Fig. 3(a) is an example of results from the two-dimensional problem (O'Malley et al.). Note that the $\log \varepsilon \to -\infty$ limit and the two-dimensional model show qualitative agreement – the pressure reaches its maximum value at the point of reattachment for example.

5. Conclusions

In this paper we have presented a new model for separated axisymmetric flow past a slender obstacle. This model is a composite of the classical Helmholtz–Kirchhoff and Prandtl–Batchelor models. It is an extension of the two-dimensional model for flow down a step presented by O'Malley et al. (1991). Indeed, because of the lack of experimental results for incompressible, axisymmetric and slender inviscid flows, the success of the two-dimensional model is the main justification for its extension to a new geometry.

We derive an integro-differential equation for the cross-sectional area of the cavity which is then analysed. Our problem contains three free parameters. For example, we could decide to choose (on the basis of some experimental results, say) to prescribe the cavity area where it joins the obstacle, the non-dimensional base pressure perturbation (from that at infinity) and the height of the equivalent afterbody. The total length of the cavity and the strength and the length of the recirculating region can, in principle, then be determined. With an afterbody present, we have shown that our model has cusped closure at the point of reattachment and hence continuity of pressure there. Finally, an explicit solution for the cavity shape and pressure distribution has been found by exploiting a large parameter in the integral equation.

The numerical solution of the integral equation can be found in a companion paper (Fitt & Wilmott (1992)). Future work will also address the question of the existence of an axisymmetric version of the Sadovskii vortex with an $O(1)$ geometry.

Acknowledgements

The authors would like to thank J.R. Ockendon, J.M. Harper and J. Norbury for helpful discussions. One of us (P.W.) is grateful for the support of the Royal Commission for the Exhibition of 1851.

References

1. K. O'Malley, A.D. Fitt, T.V. Jones, J.R. Ockendon and P. Wilmott, Models for high-Reynolds-number flow down a step. *J. Fluid Mech.* 222 (1991) 139–155.
2. M.J.M. Hill, On a spherical vortex, *Phil. Trans. R. Soc. Lond. A* 185 (1894) 213–245.
3. M.A.B. Narayanan, Y.N. Khadgi and P.R. Viswanath, Similarities in pressure distribution is separated flow behind backward-facing steps. *Aero. Q.* 25 (1974) 305–312.
4. N. Levinson, On the asymptotic shape of the cavity behind an axially symmetric nose moving through an ideal fluid. *Ann. Math.* 47 (1946) 704–730.
5. J.R. Calvert, Experiments on the flow past an inclined disk. *J. Fluid Mech.* 29 (1967) 691–703.
6. W.M. Presz and E.T. Pitkin, Flow separation near axisymmetric afterbody models. *J. Aircraft* 11 (1974) 677–682.
7. V. Atli, Wakes of four complex bodies of revolution at zero angle of attack. *AIAA J.* 27 (1989) 707–711.

8. B. Fornberg, Steady viscous flow past a sphere at high Reynolds number. *J. Fluid Mech* 190 (1988) 471–489.
9. E. Cumberbatch and T.Y. Wu, Cavity flow past a slender pointed hydrofoil. *J. Fluid Mech* 11 (1961) 187–208.
10. V.S. Sadovskii, Vortex regions in a potential stream with a jump of Bernoulli's constant at the boundary. *Z. Angew. Math. Mech.* 35 (1971) 729–735.
11. D.B. Bliss, Aerodynamic behaviour of a slender slot in a wind tunnel wall. *AIAA J.* 20 (1982) 1244–1252.
12. A.D. Fitt and P. Wilmott, A composite cavity model for axisymmetric high Reynolds number separated flow II: numerical results. In preparation (1992).
13. G.K. Batchelor, On steady laminar flow with closed streamlines at large Reynolds number. *J. Fluid Mech.* 1 (1955) 177–190.
14. S. Childress, Solutions of Euler's equations containing finite eddies. *Phys. Fluids* 9 (1966) 860–872.
15. M.J. Lighthill, A note on cusped cavities. Aeron. Res. Council Rept. & memo 2328 (1945).
16. R.A. Handelsman and J.B. Keller, Axially symmetric potential flow around a slender body. *J. Fluid Mech.* 28 (1967) 131–147.